Electronic Supplementary Information

Enhanced Charge Extraction in Organic Solar Cells through Electron Accumulation Effects Induced by Metal Nanoparticles

Feng-xian Xie,[a] Wallace C. H. Choy, *[a] Wei E. I. Sha,[a] Di Zhang,[a] Shaoqing Zhang,[b] Xinchen Li,[a] C. W. Leung,[c] and Jianhui Hou[b]

[a] *Department of Electrical and Electronic Engineering, The University of Hong Kong, Pokfulam Road, Hong Kong, (China)*
[b] *Institute of Chemistry, Chinese Academy of Sciences, Beijing 100190, (China)*
[c] *Department of Applied Physics, The Hong Kong Polytechnic University, Hung Hom, Kowloon, Hong Kong, (China)*
Corresponding author: chchoy@eee.hku.hk (Choy)

1. Au NPs, Ag NPs and TiO_2 NPs

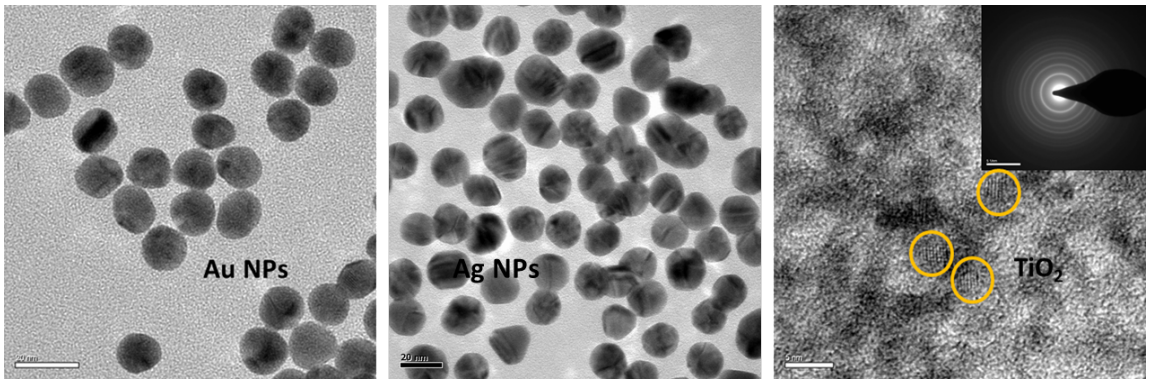

Figure. S1 Transmission electron microscopy (TEM) image of Au NPs, Ag NPs and TiO_2 NPs.

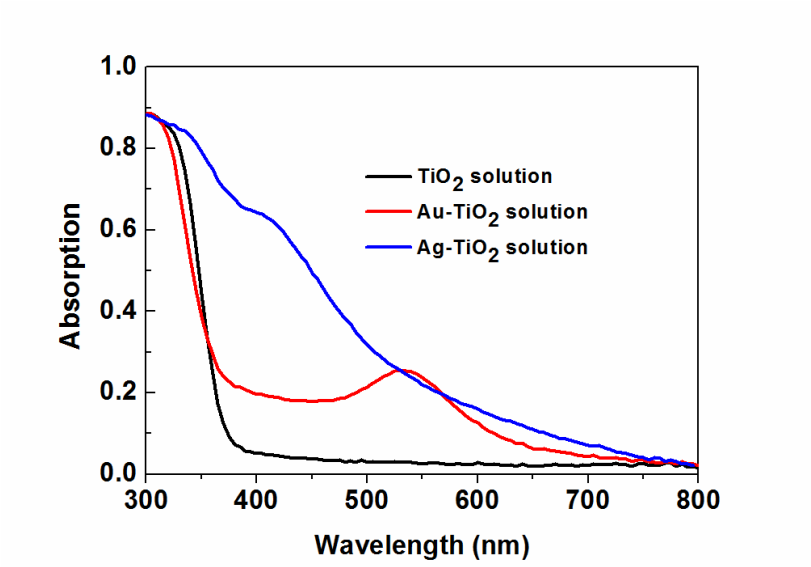

Figure. S2. Absorption Spectra of TiO_2 and Au and Ag NP-TiO_2 solutions.

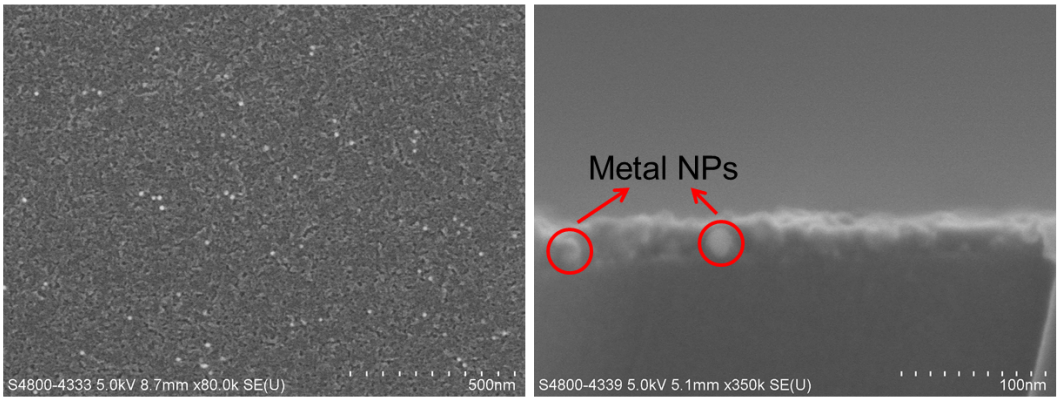

Figure. S3 (a) Top view Scanning Electron Microscopy (SEM) image and (b) cross-section SEM view of Au NP-TiO_2 composite film.

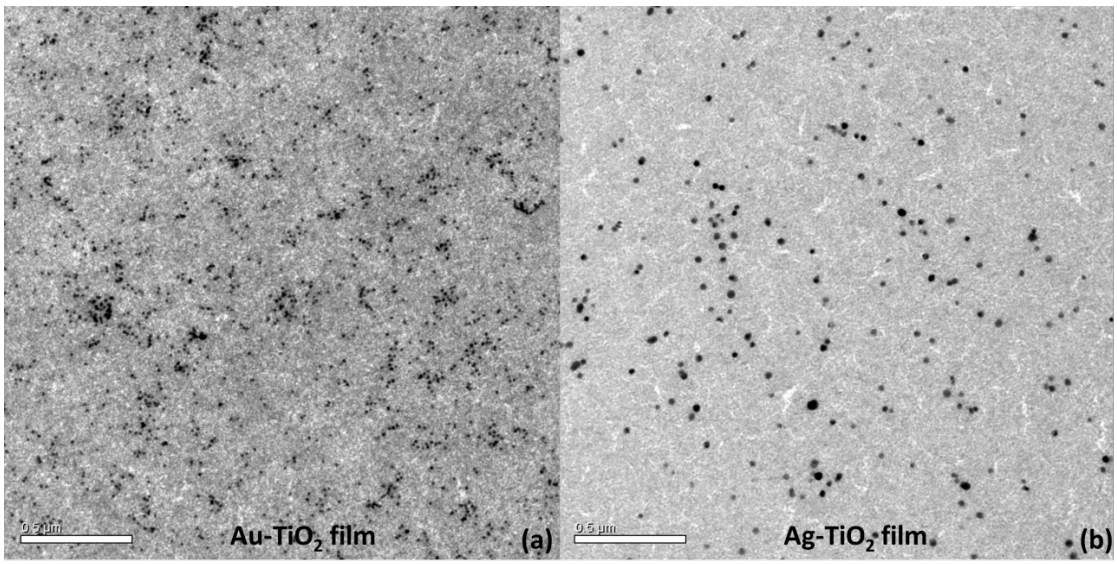

Figure. S4 Transmission electron microscopy (TEM) images of (a) Au NPs-TiO_2 film and (b) Ag NPs-TiO_2 film, spin-coated on Cu grid. (scale bar 500 nm)

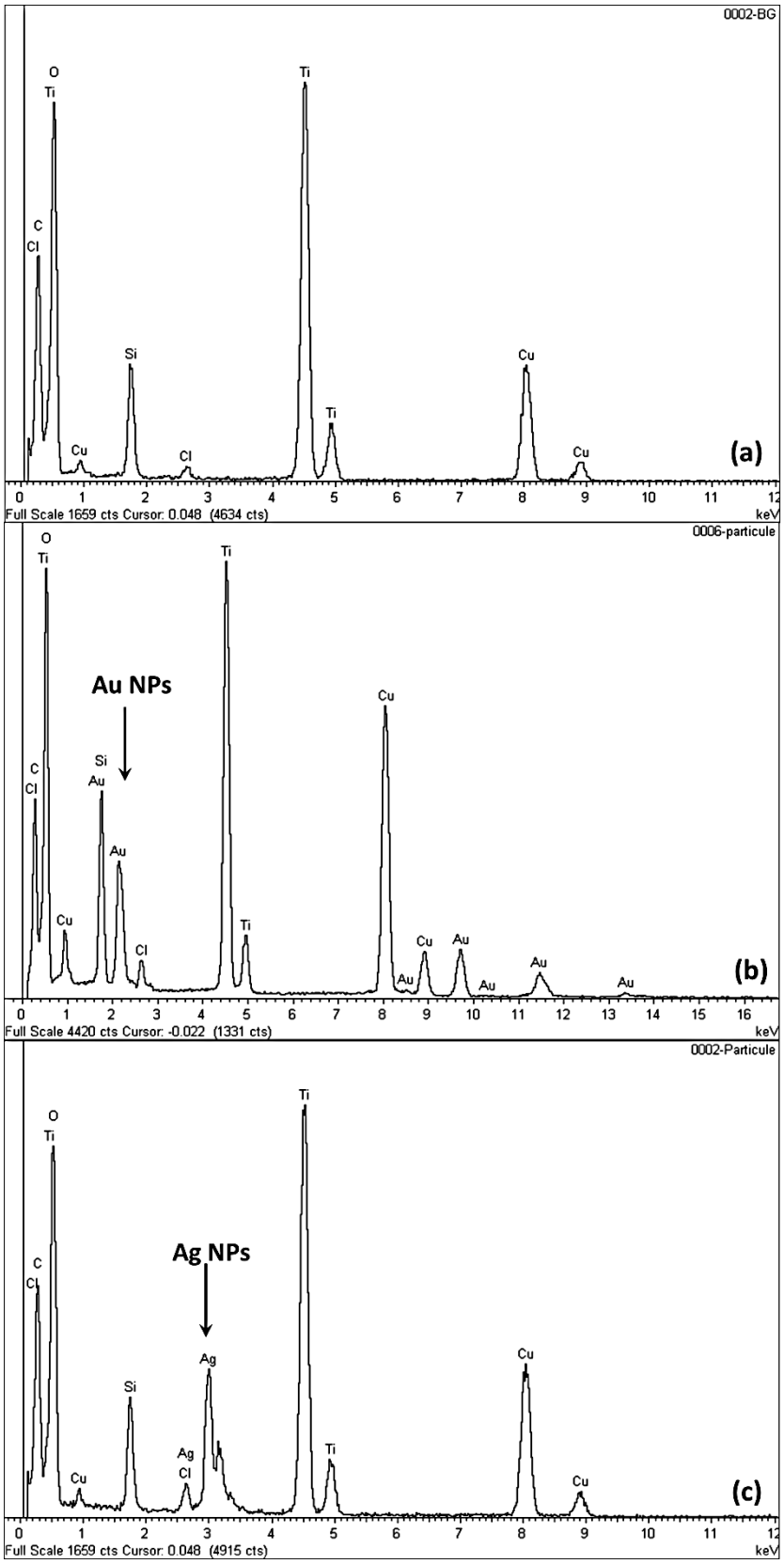

Figure. S5 EDS element spectra measured in TEM. (a) TiO_2 film, (b) Au NPs-TiO_2 film and (c) Ag NPs-TiO_2 film.

2. Effects of TiO_2 thickness on the OSC performance

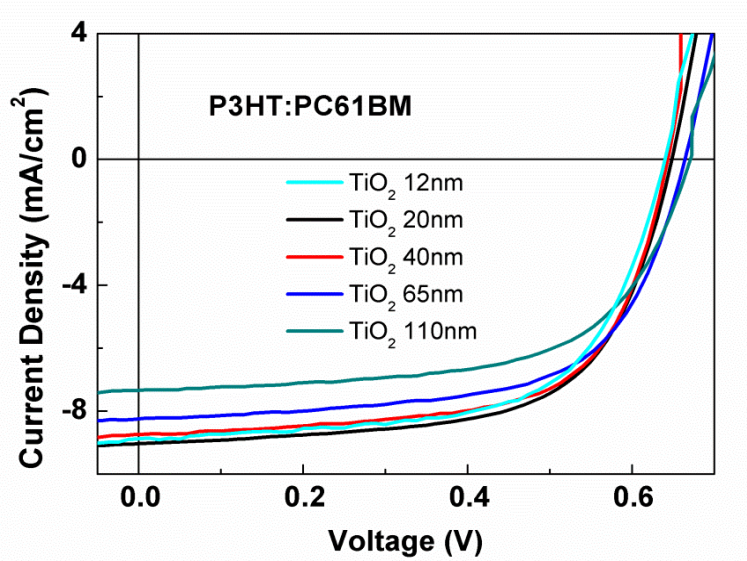

Figure. S6 *J-V* characteristics of inverted P3HT:PC_{61}BM OSCs using TiO_2 layers of different thickness as ETLs under solar illumination (AM1.5G).

Table S1. Device performance summary of inverted P3HT:PC_{61}BM OSCs using TiO_2 layers of different thickness as ETLs under solar illumination (AM1.5G).

P3HT OSCs	V_{OC}(V)	J_{SC}(mA/cm^2)	FF(%)	PCE(%)
TiO_2(12 nm)	0.636	8.90	62.8	3.56
TiO_2(20 nm)	**0.640**	**9.03**	**62.9**	**3.64**
TiO_2(40 nm)	0.645	8.75	64.3	3.62
TiO_2(65 nm)	0.659	8.29	63.3	3.45
TiO_2(110 nm)	0.672	7.35	61.2	3.03

3. Effects of metal NPs concentration on the OSC performance

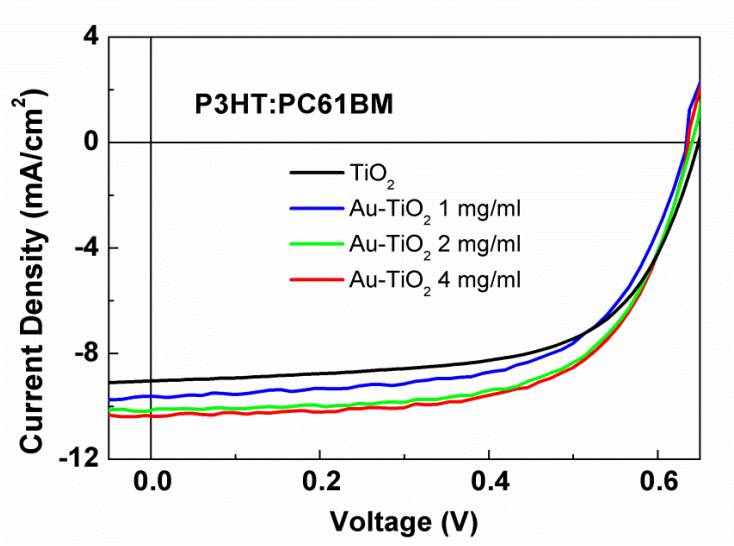

Figure. S7 *J-V* characteristics of inverted P3HT:$PC_{61}BM$ OSCs using TiO_2 and Au NP-TiO_2 (with Au NPs of different concentrations) as ETLs under solar illumination (AM1.5G). The TiO_2 solution (10 mg/ml) was mixed with different concentrations of Au NPs at volume ratio 2:1. TiO_2 film was made from diluted TiO_2 solution (10 mg/ml TiO_2 solution with ethanol at volume ratio of 2:1), with thickness of 20 nm.

Table S2 Device performance summary of inverted P3HT:$PC_{61}BM$ OSCs with TiO_2 and Au-TiO_2 (Au NPs different concentrations) as ETL under solar illumination (AM1.5G).

P3HT OSCs	V_{OC}	J_{SC}	FF	PCE
TiO_2	0.640	9.03	62.9	3.64
Au(1mg/ml)-TiO_2	0.633	9.63	63.1	3.84
Au(2mg/ml)-TiO_2	0.646	10.19	63.6	4.18
Au(4mg/ml)-TiO_2	**0.633**	**10.35**	**65.1**	**4.26**

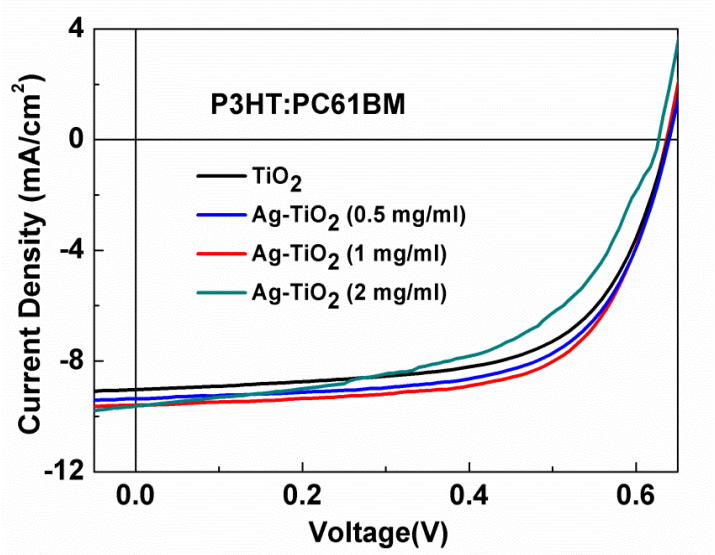

Figure. S8 *J-V* characteristics of inverted P3HT:$PC_{61}BM$ OSCs using TiO_2 and Ag NP-TiO_2 (with Ag NPs of different concentrations) as ETLs under solar illumination (AM1.5G). The TiO_2 solution (10 mg/ml) was mixed with different concentrations of Ag NPs at a volume ratio of 2:1. TiO_2 film was made from diluted TiO_2 solution (10 mg/ml TiO_2 solution with ethanol at volume ratio of 2:1), with film thickness of 20 nm.

Table S3 Device performance summary of inverted P3HT:$PC_{61}BM$ OSCs with TiO_2 and Ag-TiO_2 (Ag NPs of different concentrations) as ETL under solar illumination (AM1.5G).

P3HT OSCs	V_{OC}	J_{SC}	FF	PCE
TiO_2	0.640	9.03	62.9	3.64
Ag(0.5mg/ml)-TiO_2	0.640	9.36	64.1	3.86
Ag(1mg/ml)-TiO_2	**0.630**	**9.59**	**65.3**	**4.01**
Ag(2mg/ml)-TiO_2	0.625	9.62	54.4	3.27

4. Electron extraction enhancement in NP-TiO_2

Impedance spectroscopy measurement is conducted to investigate the charge accumulation effects of NP-TiO_2 under UV illumination, which is a powerful tool to analysis the polymer and interface properties of polymer solar cell. Nyquist plots of inverted OSCs with the pristine TiO_2 and optimized Au NP-TiO_2 layer as ETLs are shown in **Figure. S9**, measured at open-circuit voltage with and without UV excitation. **Figure. S9 (a)** shows the equivalent circuit model of the OSCs for analyzing the Nyquist plots, with the fitted equivalent circuit model composed of Rs and three components R1, R2, and R3 forming a parallel circuit with capacitors (C1, C2, and C3, respectively). The parameters of the equivalent circuit of inverted OSCs are summarized in **Table S4**. The (R1, C1) components are mainly affected by the charge extraction layers.[29, 30] The (R2, C2) component is derived from the organic active layer.[29] Extracted from the Nyquist plots, R1, R2, and R3 for the pristine TiO_2 OSC without UV excitation are 2532, 167.2, and 134.2 Ω, respectively. After UV illumination for 10 seconds, the R1, R2 and R3 values considerably decrease to 1102.0, 116.9, 72.1Ω, respectively. The reduced resistances after UV illumination is mainly due to the large number of photoconductive carriers generated in TiO_2 and the organic active layer by UV light, resulting in the decrease of CT resistance and thus

the increase of FF and PCE of the OSCs as shown from **Figure S9 (a)** to **Figure S9 (b)**. The increase of C2 in the (R2, C2) component indicates the maintaining of a large number of generated carriers under light illumination due to the low mobility of the organic materials. Interestingly, C1 component in the pristine TiO_2 OSCs remain almost unchanged after UV illumination, suggesting that only a negligible portion of photoconductive electrons remain in the TiO_2 film.

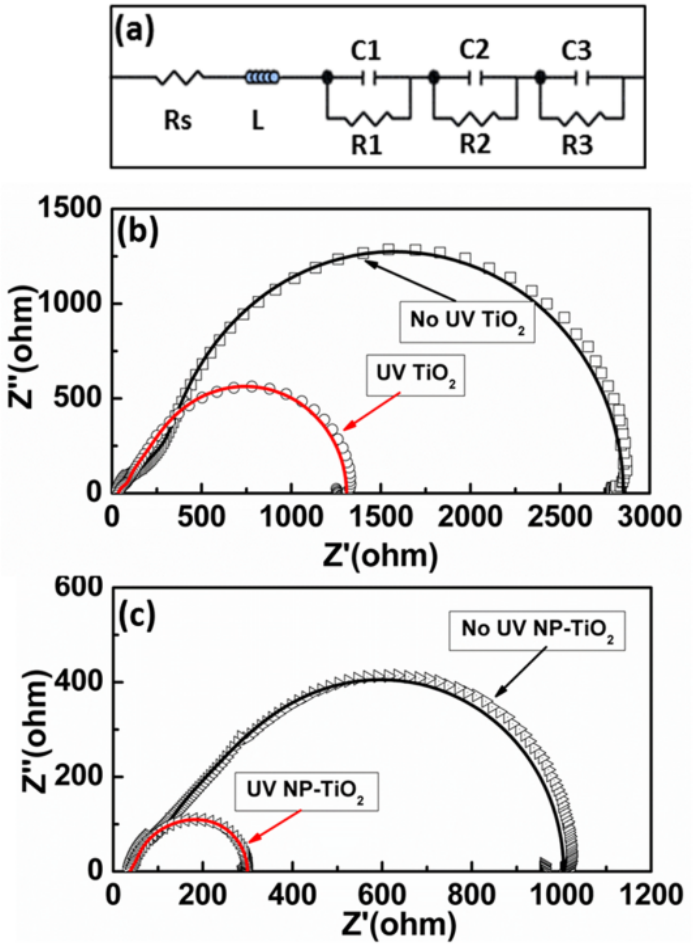

Figure. S9 (a) Equivalent circuit model for OSC devices in impedance spectroscopy measurement. (b) Nyquist plot of TiO_2 film as ETL in inverted OSCs with and without UV excitation. (c) Nyquist plot of optimized Au NP-TiO_2 film as ETL in inverted OSCs with and without UV excitation.

Table S4. Summarized Parameters of the OSC equivalent circuit with TiO_2 as ETLs measured under (a) no UV or (b) with UV excitation, and optimized Au NP-TiO_2 as ETLs measured under (c) no UV or (d) with UV excitation.

	(a)	(b)	(c)	(d)
Rs/ Ω	18.95	17.19	17.61	18.39

L1/H	1.683E-6	1.770E-6	1.599E-6	1.758E-6
R1/Ω	2532	1102	773	172
R2/Ω	167.2	116.9	119.6	75.8
R3/Ω	134.2	72.1	94.7	33.8
C1/F	1.010E-8	1.050E-8	9.127E-9	1.463E-8
C2/F	6.951E-9	1.028E-8	8.961E-9	1.057E-8
C3/F	1.063E-9	1.118E-9	1.155E-9	1.717E-9

Importantly, we observe a further decrease in the CT resistance in OSCs after UV illumination, achieved by using the NP-TiO_2 ETL. R1, R2 and R3 of NP-TiO_2 OSCs are all further decreased (to 172, 75.8 and 33.8 Ω, respectively), which are significantly smaller than those of pristine TiO_2 OSCs treated with identical UV exposure. The further reduced R1, R2 and R3 after UV illumination in NP-TiO_2 OSCs indicate additional decrease in the CT resistance introduced by the incorporated Au NPs, which is beneficial for the charge extraction in OSCs.

Meanwhile, in the impedance results, a clear increase of C1 is observed in NP-TiO_2 OSCs after UV illumination (from 9.127×10^{-9} F to 14.63×10^{-9} F), indicating accumulated negative charges in the NP-TiO_2 layer. This observation is in good agreement with the previously observed blue shift in the resonance peak wavelength of the NP-TiO_2 layer, both of which confirm the storage of UV-generated charges in the NP-TiO_2 composite by incorporating Au NPs. The occurrence of charge storage in the NP-TiO_2 composite is coupled with the enhanced OSC performance from the reduced CT resistance and improved electron extraction by the incorporation of metal NPs.